

Cite this: *J. Mater. Chem. C*, 2014, 2, 2591

Towards an understanding of structure–nonlinearity relationships in triarylamine-based push–pull electro-optic chromophores: the influence of substituent and molecular conformation on molecular hyperpolarizabilities†

Jingbo Wu, Blake A. Wilson, Dennis W. Smith, Jr. and Steven O. Nielsen*

We calculated the second-order hyperpolarizability (β) of a series of triarylamine (TAA) based donor–bridge–acceptor (D– π –A) push–pull type nonlinear optical (NLO) chromophores with different electron donor moieties and the same thiophene π -bridge and dicyanovinyl electron acceptor using a time-dependent Hartree–Fock (TDHF) approach within the software package MOPAC 2012. NLO chromophores with various quantities and positions of methoxy groups in the TAA donor moiety were investigated. The relationship between NLO properties and the electronic or geometric structures of the TAA donor subunit is discussed through the calculation results. Both substituent and conformational effects affect the delocalization of the nitrogen lone pair into the aryl rings, leading to a dramatic influence on the nonlinear optical properties. Introduction of methoxy groups at the *ortho* positions of the TAA moiety has a larger influence on the molecular hyperpolarizability and dipole moment than the introduction of methoxy group at the *para* or *meta* positions. Our calculation results demonstrate how to improve the NLO properties of TAA based chromophores while meeting practical device requirements.

Received 18th December 2013
Accepted 16th February 2014

DOI: 10.1039/c3tc32510e

www.rsc.org/MaterialsC

Introduction

Organic second-order nonlinear optical (NLO) materials have attracted a lot of attention due to their potential ultrafast switching or modulation of light in telecommunications, optical computing, and optical information processing applications.^{1–4} These practical applications require thermally and chemically robust materials with a high enough electro-optic (EO) coefficient (r_{33}) value.^{5–10} EO materials with ultrahigh nonlinear optical (NLO) response have been achieved,^{5,7,11,12} however, the thermal stability after poling of current EO materials still cannot meet the requirements for practical applications. Practical EO materials must withstand high manufacturing temperatures (250 °C or higher) for a prolonged time.^{11,12}

One class of NLO chromophores with a triarylamine (TAA) donor and a thiophene-bridge exhibits the highest thermal stability of all reported chromophores,^{13–16} which seems to be the best candidate for the active EO materials in a practical device. However, compared to their alkyl counterparts, TAA based chromophores usually exhibit reduced hyperpolarizabilities due to

delocalization of the nitrogen lone pair into the two phenyl rings which do not connect with the bridge⁸ and a lower EO coefficient, which may be due to π – π stacking interactions and charge transport between chromophores.^{10,14} This encouraged us to modify TAA based chromophores to improve their hyperpolarizabilities and thus overcome their drawbacks while maintaining high thermal stability. In order to optimize NLO chromophore hyperpolarizability, significant theoretical and experimental efforts have been focused on modifying conjugated bridges^{17–24} and the structure of electron acceptors.²⁵ However, very little experimental and theoretical efforts have been directed to the investigation of the electron donor moiety.^{10,26–29} To the best of our knowledge, a detailed understanding of the relationship between NLO properties and the electronic and geometric structures of the TAA donor subunit of chromophores is lacking.

In this paper, we present a systematic computational study of a series of model chromophores with different numbers and positions of methoxy groups in the TAA donor moiety. All designed model chromophores have the same thiophene-bridge and a simple dicyanovinyl electron acceptor. Our results reveal that the substituent and the molecular conformation of the TAA donor moiety in NLO chromophores dramatically affect their nonlinear optical properties. In a properly designed system, significant enhancement in the hyperpolarizability of TAA based NLO chromophores can be achieved compared to unsubstituted TAA chromophores.

Department of Chemistry, The University of Texas at Dallas, Richardson, TX 75080, USA. E-mail: steven.nielsen@utdallas.edu; Fax: +1 972 883 2925; Tel: +1 972 883 5323

† Electronic supplementary information (ESI) available: All input files of model chromophores and all calculation results. See DOI: 10.1039/c3tc32510e

Background

Earlier experimental and theoretical studies on the structure of triarylamine molecule afford several significant observations.^{30–33} Firstly, the delocalization of the nitrogen lone pair into the phenyl rings is strongly influenced by the molecular conformation and electronic character of the three phenyl rings.^{34–36} Secondly, the structure of the central NCCC moiety is planar or near planar. (Fig. 1(I)) Introduction of one or multiple substituent groups in the different positions of the phenyl ring does not influence the planar conformation of the central NCCC moiety significantly.^{35,36} Thirdly, the three phenyl rings are symmetrically twisted from the central NCCC plane and present a compromised structure between two opposing forces. Those are the energy-lowering conjugation between the π -electrons of the phenyl groups and the central lone pair of nitrogen, and the energy-increasing repulsion between hydrogen atoms of neighbouring phenyl rings.³⁰ Each phenyl ring forms a certain torsion angle with the central reference plane. The experimental data shows this torsion angle is $41\text{--}44^\circ$ in gaseous phase.³¹ Our calculations show this torsion angle is appropriate 35° . The torsion angle is a key conformational parameter and provides us with quantitative information on the molecular conformation of TAA donor moieties. Finally, the di-*ortho* substituted TAA molecule has a dramatically different molecular conformation compared to the natural TAA.³⁶ The observed structure of dimethoxy *ortho*-substituted TAA shows the unsubstituted phenyl ring lies close to the central trigonal plane, while the other two substituted phenyl rings are almost orthogonal to the central reference plane (Fig. 1(II)).

In second-order NLO materials, the second order polarizability β is associated with intramolecular charge transfer (ICT) from the nitrogen lone pair to the acceptor through a π -conjugated bridge. The ICT is influenced by the character of the lone electron pair on the N atom. Increasing the electron density of the electron donor enhances the hyperpolarizability. Previous studies show that introduction of methoxy groups on the *para* positions of the TAA donor moiety can increase the electron density of the donor and enhance the hyperpolarizability.^{13–16} However, other positions for substituted groups in the TAA moiety of NLO chromophores, especially the *ortho* position, have not yet been studied. Moreover, due to the character of the lone electron pair on the N atom being strongly influenced by the molecular conformation, we hypothesize the molecular conformation should strongly affect the hyperpolarizability, which also has not yet been studied.

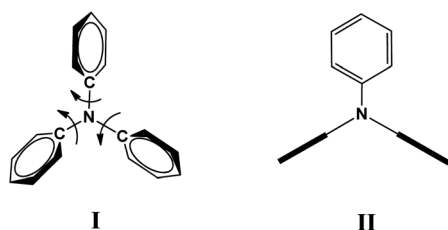


Fig. 1 The structure of TAA with three rotatable phenyl rings (I) and an important molecular conformation of triarylamine (II).

Structure entry and computational methods

The structures of the molecules were sketched using the ChemDraw Ultra 12.0 program in ChemBiooffice2012.³⁷ By comparing with previous experimental crystal structures, the three-dimensional (3D) geometries were preoptimized by running the MM2 energy-minimization and manually changed by the rotation of acceptor, thiophene ring, and ethylenic moieties in the Chem3D Pro program to ensure that low-energy conformations were obtained. The resulting geometry of each structure was converted into a MOPAC input file. Geometry optimizations were performed using the AM1 Hamiltonian in the MOPAC 2012 software package. Each final optimized structure was verified as an energy minimum on the potential energy hypersurface by calculation of the harmonic vibrational frequencies; no imaginary frequencies were discovered. The second-order average hyperpolarizabilities (β) were calculated at 1907 nm (0.65 eV) for the AM1 optimized geometries using the default time-dependent Hartree-Fock (TDHF) method.³⁸ In order to understand the structure-property relationship, important parameters such as the average dipole moment (μ), total energy (E), static and frequency dependent average polarizability (α), second-order average hyperpolarizability at 1907 nm (β_{1907}), highest occupied molecular orbital (HOMO) and lowest occupied molecular orbital (LUMO) energies, three C–N bond lengths, and three torsion angles of the three phenyl rings with the central plane of the NCCC moiety ($\angle A$, $\angle B$, and $\angle C$) were calculated, respectively. The TDHF method is considered reliable in predicting trends in hyperpolarizability, but the absolute magnitude of the computed hyperpolarizabilities should not be thought of as being highly accurate or directly comparable with experimental data.^{18,26}

Visual Molecular Dynamics (VMD)³⁹ was used to visualize the molecular coordinates and subsequently calculate the torsion angle values. The torsion angle between two separate planes within a molecule was determined by selecting three atoms from each plane. The three atoms from each plane were then used to determine a unit normal vector for each plane. The minimum angle between the two unit normal vectors was then determined and taken as the torsion angle, such that the torsion angle lies in the range from 0 to 90 degrees.

The molecular geometries of several model chromophores originally came from the MOPAC calculation and were fully optimized at the density functional B3LYP/6-31G (d) level using the Gaussian 03W⁴⁰ package. Isosurfaces of the HOMO and LUMO for these model chromophores were calculated with B3LYP/6-31G (d).

Results and discussion

Understanding several basic facts of NLO chromophores

Previous theoretical studies showed that the different rotational isomers of NLO chromophores exhibited different hyperpolarizabilities.⁴¹ We first investigated this observation in order to find the rotational isomer with the highest hyperpolarizability. The geometry optimized structure of chromophore 3 is shown in

Fig. 2. Three rotational chromophore isomers **1–3** (Scheme 1) were created by rotating the single bonds between the thiophene and vinyl groups in the backbone, and their hyperpolarizabilities were then calculated. Our calculation results were consistent with previous studies showing that the relative conformations of vinyl and thiophene groups affect the hyperpolarizabilities of EO chromophores. These three isomers have almost identical total energy, and display a small difference in dipolar moments (*i.e.* $1 < 2 < 3$) and hyperpolarizabilities (*i.e.* $1 < 2 < 3$). Chromophore **3** has the highest hyperpolarizability among these three conformational isomers, where all model chromophores we study have

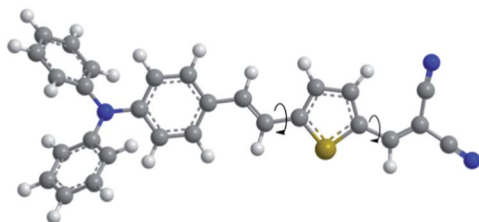
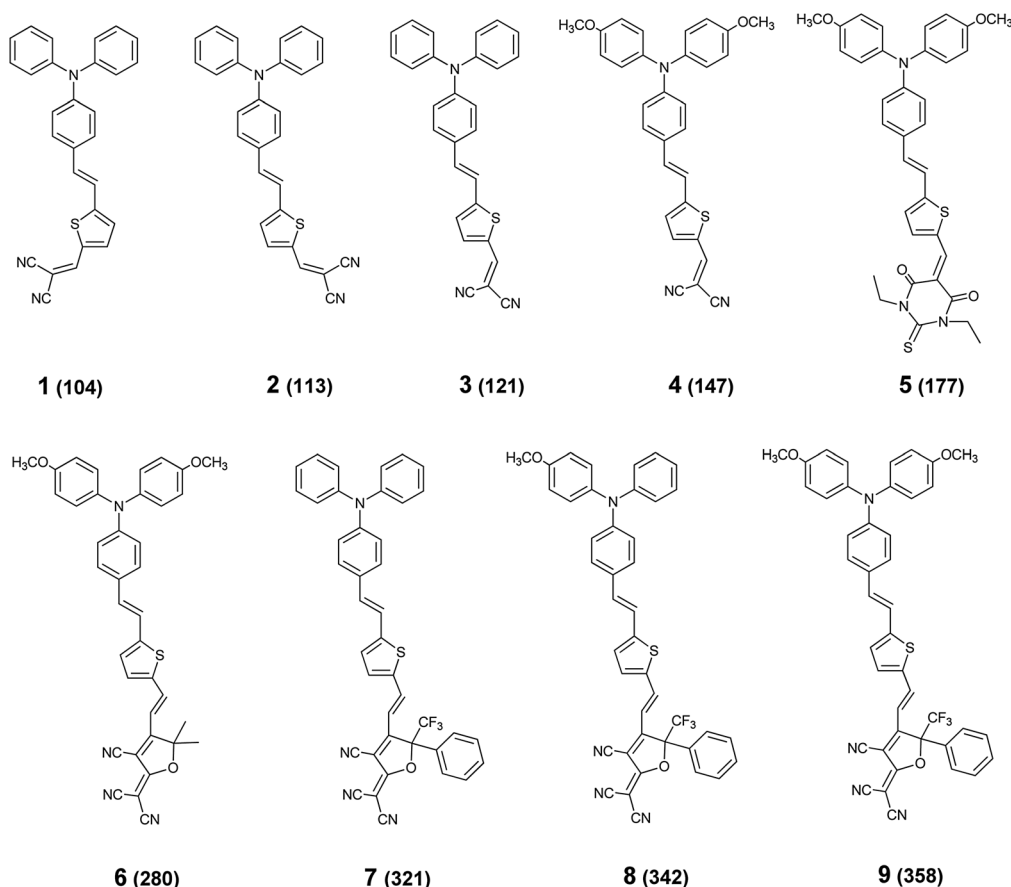


Fig. 2 The geometry optimized structure of model NLO chromophore **3**. Three conformational isomers can be created by rotation of the single bonds between the vinyl groups and the thiophene ring in the backbone.

the same conformation between the thiophene and vinyl groups as chromophore **3**.

Several published TAA based EO chromophores used for our tests are illustrated in Scheme 1. They have the same thiophene π -bridges. Unsubstituted, mono-methoxy *para*-substituted, and di-methoxy *para*-substituted triarylamines are chosen as electron donors. Four different electron acceptors, dicyanovinyl (**4**), barbituric acid (BBA, **5**), 2-(3-cyano-4,5,5-trimethyl-5*H*-furan-2-ylidene)-malonitrile (TCF, **6**) and 2-dicyanomethylene-3-cyano-4-methyl-5-trifluoromethyl-5-phenyl-2,5-dihydrofuran (CF_3 -phenyl-TCF, **7–9**) are shown. The hyperpolarizability β values of chromophores **4–9** have been measured in solvent.^{14,16} The EO coefficient (r_{33}) values of chromophores **7–9** in the guest and host systems have been measured.¹⁴ The average second-order molecular hyperpolarizability β values calculated at 1907 nm (0.65 eV) by the AM1/TDHF method are listed in parentheses in Scheme 1, with all other details provided in the ESI.†

Our calculations show the NLO chromophores with a di-methoxy substituted TAA donor group display larger hyperpolarizabilities than their analogues with an unsubstituted TAA donor group (*cf.* **3** vs. **4**, and **7** vs. **8**). The di-methoxy *para*-substituted TAA based chromophore has a larger β value than the mono-methoxy *para*-substituted analogues. Increasing the number of methoxy groups on the *para*-position of the TAA



Scheme 1 The structures of three conformational isomers and several reported TAA based NLO chromophores. Numbers in parentheses are β_{1907} value in units of 10^{-30} esu.

donor moiety will yield an increase in hyperpolarizability (cf. 8 vs. 9). These trends in hyperpolarizability predicted by our calculations are consistent with previous experimental results.^{14,16}

EO chromophores with stronger electron acceptor groups display larger hyperpolarizabilities than their analogues with weaker electron acceptor groups. In the di-substituted TAA-thiophene series, hyperpolarizabilities increase in the order of $4 < 5 < 6 < 9$. This trend in hyperpolarizability predicted by our calculations is consistent with experimental results and the trend in the strength of electron acceptor groups.

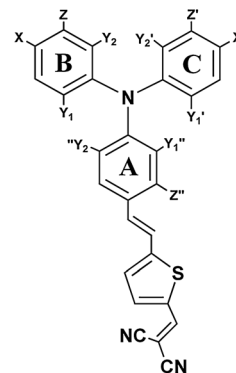
The absolute magnitude of hyperpolarizabilities from quantum calculations carried out in the gas phase is not considered accurate or directly comparable with experimental data which are measured in solvent, such as CHCl_3 . For example, our calculation of the β value at 1907 nm in vacuum for chromophore 9 is only 357×10^{-30} esu and the experimental β value at 1907 nm in CHCl_3 is 3456×10^{-30} esu.¹⁴ However, our calculation results are considered reliable in predicting trends in hyperpolarizability. The predicted trends in hyperpolarizabilities from calculation results and from available experimental data are compared in the ESI.†

Substituted triarylamine moieties

It was reported that introduction of methoxy groups into *para* positions of the TAA moiety of EO chromophores increases their hyperpolarizability. However, the influence of the position and number of methoxy groups in TAA donor moieties on the hyperpolarizabilities of NLO chromophores have not been studied yet. In this study, a variety of model chromophores containing triarylamine moieties with different numbers and positions of methoxy groups and the same thiophene bridge and dicyanovinyl electron acceptor are designed. The average second-order molecular hyperpolarizability values calculated at 1907 nm (0.65 eV) by the AM1/TDHF method are listed in Scheme 2, with all other details in the ESI.†

The key findings revealed in Scheme 2 are: (1) introduction of methoxy groups on the *ortho* positions of TAA donor moieties dramatically impacts the molecular conformations of the TAA donor moieties, the hyperpolarizabilities, and the dipole moments; (2) introduction of additional methoxy groups on *para* and *ortho* positions of ring B and ring C in the TAA donor moiety results in larger hyperpolarizabilities; (3) the hyperpolarizability and dipole moment were enhanced by simply introducing a methoxy group on the *meta* position of the phenyl ring connected to the bridge; and (4) the influence of substitution at the different positions on the molecular conformation of the TAA donor moiety increases in the order: *ortho* > *para* > *meta*.

Model chromophores (10–14) with only one methoxy substituent at five different positions on the TAA moiety were investigated. The three phenyl rings are labelled using three letters: A, B, and C. Phenyl ring A conjugates with the π -bridge and the dicyanovinyl electron acceptor. Our calculation results show that introduction of a methoxy group on ring B or C in a position *para*- or *ortho*- to the amine N centre improves hyperpolarizabilities of EO chromophores whereas in a position *meta*-



model	substituents	β_{1907}
		10^{-30} esu
3	none	121
10	X = OMe (<i>para</i>)	131
11	Y = OMe (<i>ortho</i>)	131
12	Z = OMe (<i>meta</i>)	104
13	Y ₁ '' = OMe (<i>ortho</i>)	69
14	Z'' = OMe (<i>meta</i>)	127
4	X = X' = OMe	147
15	Y ₁ = Y ₁ ' = OMe (<i>trans</i>)	172
16	Y ₁ = Y ₁ ' = OMe (<i>cis</i>)	159
17	Y ₁ '' = Y ₂ '' = OMe	43
18	Z = Z' = OMe	111
19	Y ₁ = Y ₂ = Y ₁ ' = Y ₂ ' = OMe	183
20	X = X' = Y ₁ = Y ₁ ' = OMe	185
21	X = X' = Y ₁ = Y ₂ = Y ₁ ' = Y ₂ ' = OMe	199
22	X = X' = Y ₁ = Y ₂ = Y ₁ ' = Y ₂ ' = Z'' = OMe	216
32	X = X' = N(CH ₃) ₂ ; Y ₁ = Y ₂ = Y ₁ ' = Y ₂ ' = Z'' = OMe	247

Scheme 2 The structures of methoxy and hybrid substituted TAA based NLO chromophores and their β_{1907} values.

to the amine N centre slightly decreases hyperpolarizabilities. Introduction of a methoxy group on ring A in a position *ortho*- to the central N atom dramatically decreases the hyperpolarizability. Introduction of a methoxy group on ring A in a position *meta*- to the amine nitrogen centre yields a small increase in the hyperpolarizability and an obvious increase in the average dipolar moment. In summary, hyperpolarizability β_{1907} values are in the trend of $10 \approx 11 > 14 > 3 > 12 > 13$.

For chromophore 10, *para*-substitution has a slight influence on the molecular conformation of the TAA donor moiety because the torsion angles of the three phenyl rings change very little compared to that of the unsubstituted TAA moiety. The enhanced hyperpolarizability largely comes from the electron donor effect by π -interaction with the oxygen lone pair.

For mono-*ortho*-substituted chromophore 11, the molecular conformation of the TAA donor moiety changed significantly and dramatically affected the π -interaction between the oxygen lone pair and central N lone pair. The torsion angle between ring B and the central reference plane is 78° , which dramatically decreases the delocalization of the nitrogen lone pair into ring B (enhanced β_{1907} value) and reduces the electron donor effect from the oxygen lone pair through π -interaction (decreased β_{1907} value). The small decrease in torsion angle between ring A and the central reference plane causes slightly better delocalization of the nitrogen lone pair into ring A. Overall,

chromophore **10** ($\beta_{1907} = 131 \times 10^{-30}$ esu) and chromophore **11** ($\beta_{1907} = 131 \times 10^{-30}$ esu) display similar β_{1907} values, however, the *ortho*-substituted chromophore **11** has a larger dipolar moment value (cf. **10**, $\mu = 6.6$ D vs. **11**, $\mu = 8.4$ D). The conformation of the TAA moiety affects the average dipolar moment of the chromophore.

The torsion angles of the three phenyl rings of *meta*-substituted chromophore **12** are similar to those of non-substituted chromophore **3**, which shows that the molecular conformation of the TAA donor moiety does not change. Because the methoxy group is located at the *meta* position to the central N atom, no electron donating effect from π -interaction with the oxygen lone pair occurs. An induced effect from the higher electronegative oxygen causes a small decrease in hyperpolarizability.

Introduction of a methoxy group on the *ortho* position of ring A in chromophore **13** forces ring A to rotate out of the central reference plane. The torsion angle between ring A and the central reference plane increases to 51° , which reduces the delocalization of the nitrogen lone pair into ring A and causes a large decrease in hyperpolarizability and dipole moment. The longer N–C_{ring A} bond length (1.422 Å) also supports this conclusion.

Introduction of a methoxy group on the *meta*-position of ring A yields a small increase in hyperpolarizability (cf. **14** vs. **3**), and an obvious increase in dipole moment (cf. **14**, $\mu = 8.5$ D vs. **3**, $\mu = 6.9$ D). This enhanced hyperpolarizability and dipole moment by introducing an extra electron donor group in the *meta*-position of ring A is consistent with previous studies.²⁶ In the geometry optimized structure of chromophore **14**, we find the oxygen atom in the methoxy group forms a hydrogen bond with the vinyl hydrogen. (Fig. 3, the O...H distance is 2.29 Å) This hydrogen bond may stabilize the vinyl bond conformation, which may also contribute to the increase in hyperpolarizability and dipole moment.

To further understand the structure and NLO property relationship, di-methoxy substituted TAA derivatives were investigated. Di-methoxy *para*-substituted chromophore **4** displays a higher hyperpolarizability and larger dipole moment than monomethoxy *para*-substituted chromophore **10**, which is consistent with previous studies. To our surprise, the di-methoxy *ortho*-substituted chromophore **15** ($\beta_{1907} = 172 \times 10^{-30}$ esu, $\mu = 9.9$ D) displays a larger hyperpolarizability and dipole moment than those of di-methoxy *para*-substituted

chromophore **4** ($\beta_{1907} = 147 \times 10^{-30}$ esu, $\mu = 8.1$ D). Chromophore **15** and chromophore **4** have similar electron factors; however, they have an obvious difference in the molecular conformation of the TAA donor moiety. In *ortho*-substituted chromophore **15**, the torsion angles of ring B and ring C increase to 85° and 90° , respectively. Ring B and ring C are almost orthogonal to the central NCCC plane (Fig. 4). Ring A lies almost in the central plane of the NCCC moiety, with the torsion angle of ring A being just 3° . Again, in this conformation, the lone electron pair of the central N atom favours delocalization into the electron acceptor through ring A and the thiophene bridge, with minimal delocalization into the other two phenyl rings. Furthermore it has a minimal electron donor effect from the oxygen lone pair through π -interaction. This conformational effect mainly contributes to the large difference in hyperpolarizability and dipole moment between chromophore **15** and **4**.

By carefully controlling the preoptimized structures, the geometry optimized structures of two conformational isomers of the di-*ortho* methoxy-substituted chromophore, **15** and **16**, are achieved. For chromophore **15**, the two methoxy groups adopt a “*trans*” geometry, that is, the two methoxy groups are located on different sides of the NCCC plane (Fig. 4). For chromophore **16**, the two methoxy groups adopt a “*cis*” geometry, that is, the two methoxy groups are located on the same side of the central NCCC plane (Fig. 4).³⁶ The hyperpolarizability of “*trans*” chromophore **15** ($\beta_{1907} = 172 \times 10^{-30}$) exceeds that of “*cis*” chromophore **16** ($\beta_{1907} = 159 \times 10^{-30}$) due to the difference in molecular conformation. For chromophore **15**, the lone electron pair of the central N atom has more delocalization into the electron acceptor through ring A and the thiophene bridge and less delocalization into the other two phenyl rings. The structure of the TAA moiety in chromophore **15** is similar to the crystal structure of the di-*ortho* methoxy-substituted triarylamine molecule.³⁶

Introduction of two methoxy groups at both *ortho* positions of ring A (cf. **17** vs. **13**) causes ring A to twist out of the central NCCC plane. The torsion angle of ring A is 86° in chromophore **17**, which shows that ring A is almost orthogonal to the central NCCC plane (Fig. 5). In this conformation, the electron lone pair of the central N atom minimally delocalizes into ring A and the electron acceptor, which yields a large decrease in the hyperpolarizability and dipole moment. From the relative β_{1907} values

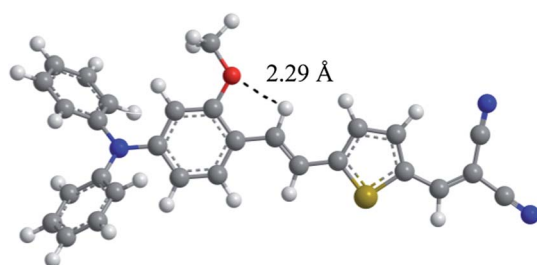


Fig. 3 The geometry optimized structure of chromophore **14**. The hydrogen bond between the oxygen atom in the methoxy group and the vinyl hydrogen has an O...H distance of 2.29 Å.

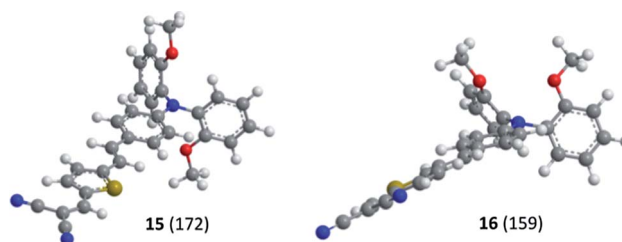


Fig. 4 The geometry optimized structures of di-methoxy *ortho*-substituted isomers, chromophore **15** (“*trans*” conformation) and chromophore **16** (“*cis*” conformation). Numbers in parentheses are β_{1907} values in units of 10^{-30} esu.

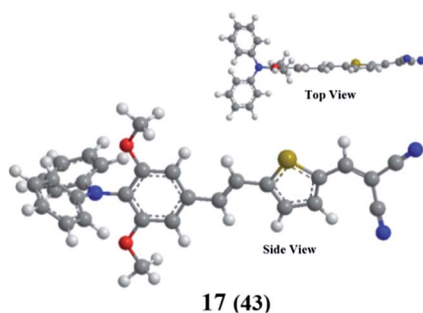


Fig. 5 The geometry optimized structure of chromophore 17 with di-methoxy *ortho*-substituted ring A. The number in parentheses is the β_{1907} value in units of 10^{-30} esu.

of chromophore 17 ($\beta_{1907} = 43 \times 10^{-30}$ esu) and chromophore 13 ($\beta_{1907} = 69 \times 10^{-30}$ esu), we can conclude that larger torsion angles of ring A yield larger decreases in hyperpolarizability.

Di-methoxy *meta*-substituted TAA chromophore 18 and mono-methoxy *meta*-substituted TAA chromophore 12 have subtle differences in hyperpolarizability and dipole moment. The torsion angles of the three phenyl rings and other parameters of chromophore 18 and chromophore 12 are similar to each other. Introduction of two methoxy groups on the *meta* positions of the TAA donor moiety does not have a substantial influence on hyperpolarizability.

For chromophore 19 (Fig. 6), all four *ortho* positions of ring B and ring C were substituted by methoxy groups. Chromophore 19 has a similar molecular conformation with chromophore 16. Introduction of two more methoxy groups on the *ortho* positions of the TAA donor moiety yields a clear increase in molecular hyperpolarizability (cf. 19, $\beta_{1907} = 183 \times 10^{-30}$ esu vs. 16, $\beta_{1907} = 159 \times 10^{-30}$ esu) and dipole moment (cf. 19, $\mu = 12.4$ D vs. 16, $\mu = 9.8$ D). Introduction of more methoxy groups on the *ortho*

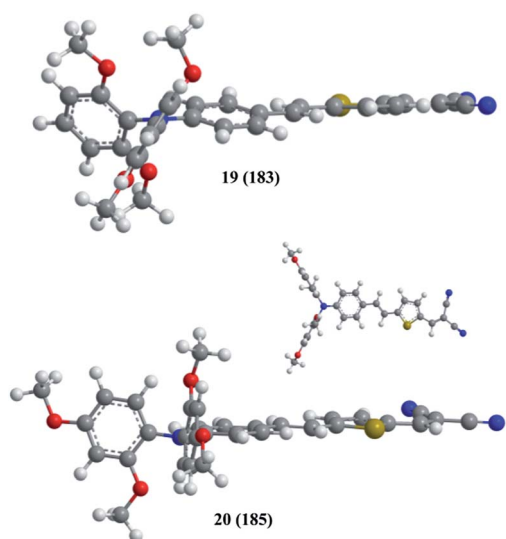


Fig. 6 The geometry optimized structures of tetra-methoxy substituted isomers, chromophore 19 and chromophore 20, show two different conformations of the TAA moiety. Numbers in parentheses are β_{1907} values in units of 10^{-30} esu.

positions of ring B or ring C has a large influence on both hyperpolarizability and dipole moment.

For chromophore 20, two methoxy groups are on *ortho* positions and two methoxy groups are on *para* positions of ring B and C of the TAA donor moiety, respectively (Fig. 6). Chromophore 20 has a similar molecular conformation with chromophore 15. Introduction of two more methoxy groups on the *para* positions of the TAA donor moiety yields an obvious increase in molecular hyperpolarizability (cf. 20, $\beta_{1907} = 185 \times 10^{-30}$ esu vs. 15, $\beta_{1907} = 172 \times 10^{-30}$ esu) and a slight increase in dipole moment (cf. 20, $\mu = 10.3$ D vs. 16, $\mu = 9.9$ D).

The electronic effect mainly contributes to the enhanced hyperpolarizability of the two pairs of chromophores. (cf. 3 vs. 4 and 15 vs. 20) The difference in β_{1907} value between chromophore 4 and chromophore 3 is 26×10^{-30} esu. The difference in β_{1907} value between chromophore 20 and chromophore 15 is 13×10^{-30} esu. The main difference between these two pairs of chromophores is the molecular conformation of the TAA moiety. Increasing the torsion angle between the central NCCC plane and ring B or ring C reduces the electronic donor effect.

Chromophore 21 with all *para* and *ortho* positions substituted with methoxy groups on ring B and ring C in the TAA donor moiety has a similar molecular conformation with chromophore 19. The enhanced hyperpolarizability comes from the electron donor effect of two extra methoxy groups on the *para* position of ring B and ring C. *Para* substitution has a minor effect on molecular dipole moment.

Chromophore 22 with all *para* and *ortho* positions substituted with methoxy groups on ring B and ring C and a methoxy group on the *meta*-position of ring A in the TAA donor moiety gives the highest dipole moment (μ) and hyperpolarizability (β_{1907}) values of all methoxy substituted model chromophores, with a dramatically enhanced β_{1907} value compared with nonsubstituted chromophore 3 (increase of about 79%). Both electron donor substituent and conformational effects play an important role in determining the hyperpolarizabilities of EO chromophores.

Several EO model chromophores with different numbers and positions of dimethylamino groups in the TAA donor moiety were also designed and studied. We observed effects similar to the methoxy group. The dimethylamino group has a better electron donor effect on *para* positions. However, introduction of dimethylamino groups on the *ortho* positions of the TAA moiety has a diminished conformational effect compared to that of methoxy groups. Taking advantage of both methoxy and dimethylamino groups, chromophore 32 with two dimethylamino groups on the *para* positions of ring B and ring C, four methoxy groups on the *ortho* positions of ring B and ring C, and one methoxy group on the *meta* position of ring A gives the highest β_{1907} value and dipolar moment of all designed model molecules (see ESI† for details).

Frontier molecular orbits

To visually understand the relationship between the NLO properties and the structures, the frontier molecular orbitals of model chromophores 3, 4, 15, 16, 20, and 22 were calculated.

The molecular geometries of these model chromophores originally came from the MOPAC calculation and were fully optimized at the density functional B3LYP/6-31G (d) level using the Gaussian 03W package. Chromophore 3 with a nonsubstituted TAA moiety has the lowest torsion angles between ring B and ring C and the central NCCC reference plane. Di-methoxy substituted chromophore 4, 15, and 16 have different torsion angles between ring B or ring C and the central NCCC reference plane. Chromophore 20 has a similar conformational structure of the TAA moiety with chromophore 15. Chromophore 22 has the highest hyperpolarizability and maximal numbers of methoxy groups on the TAA moiety.

As shown in Fig. 7, isosurfaces of the HOMOs and LUMOs for model chromophores 3, 4, 15, 16, 20 and 22 were plotted. The HOMO electronic cloud is condensed around the central NCCC moiety. Increasing the torsion angles between ring B or ring C and the central NCCC moiety leads to less delocalization of the HOMO over both phenyl rings B and C. Chromophores 3 and 4 have smaller torsion angles and display the largest delocalization of the HOMO over phenyl rings B and C. Chromophore 15 has maximal torsion angles and displays minimal delocalization of the HOMO over phenyl rings B and

C. For chromophore 20, the electron donor effect from two extra methoxy group on *para* positions of ring B and ring C mainly contribute to the enhanced hyperpolarizability compared to chromophore 15. The LUMO electronic cloud is condensed mostly on the thiophene bridge and electronic acceptor.

The HOMO distributions on the substituted ring B or ring C of chromophore 15, 16, 20 and 22 are shown in Fig. 8. Chromophore 15 has a similar molecular conformation of the TAA moiety with chromophore 20, and chromophore 16 has a similar molecular conformation of the TAA moiety with chromophore 22. To our surprise, in the HOMOs of model chromophore 15 and chromophore 20, there are no or little contributions from the lone pair electron on the oxygen atoms in *ortho*-substituted methoxy groups on phenyl ring B and ring C. The main reason is that the conformational factor effectively reduces delocalization of the lone pair of the O atom of the two methoxy groups. Only the conformational factors contribute to the enhanced hyperpolarizability, and there is no contribution from electron donor effects. In the HOMO of chromophore 16, the two *ortho*-substituted methoxy groups adopt a “*cis*” geometry, and there exist contributions from the lone pair electron of oxygen atoms. In the HOMO of chromophore 20, there is no or little contribution from oxygen atoms of methoxy groups on the *ortho* positions of ring B and ring C, and some contribution from oxygen atoms of methoxy groups on the *para* positions of ring B and ring C. In the HOMO of chromophore 22, there exist contributions from the lone pair electron of oxygen atoms in all substituted positions in the TAA moiety. Furthermore the torsion angles between the central NCCC moiety and phenyl rings B and C of chromophore 22 are larger than those of unsubstituted chromophore 3. Both an electron-donating effect from oxygen atoms and a conformational effect from steric factors contribute to the larger increase in hyperpolarizability. Chromophore 22 has the highest β_{1907} value of all methoxy substituted model chromophores.

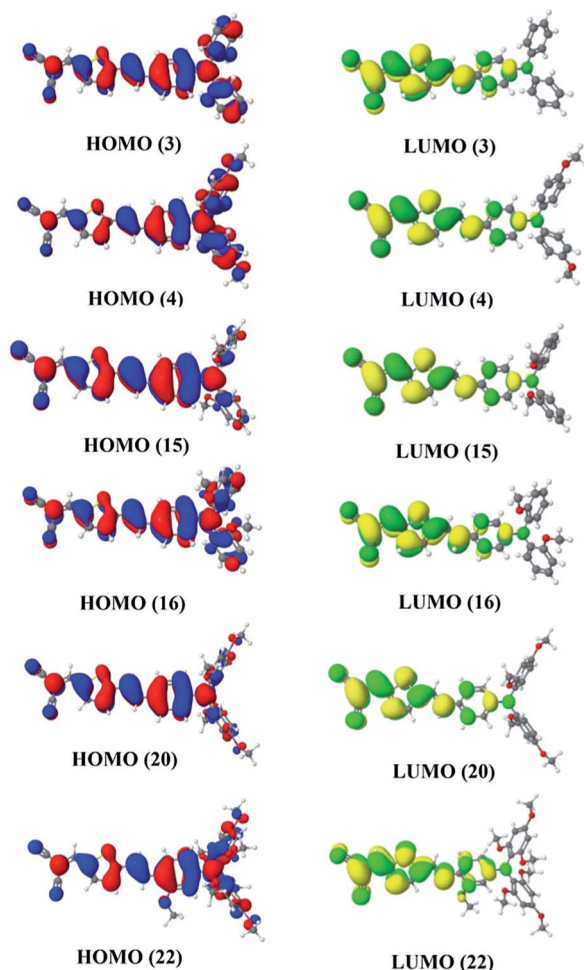


Fig. 7 The frontier molecular orbitals (HOMO and LUMO) of model NLO chromophores 3, 4, 15, 16, 20 and 22.

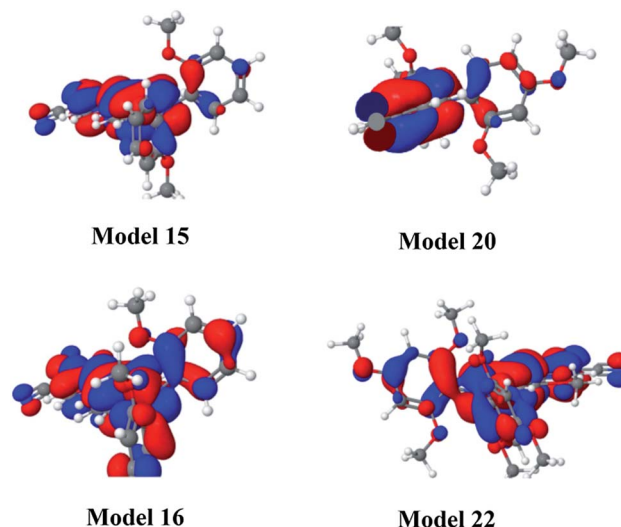


Fig. 8 Isosurfaces of the HOMO for phenyl ring B or phenyl ring C in the TAA moiety of model NLO chromophores 15, 16, 20 and 22.

Conclusions

In order to better understand the relationships between the structures and nonlinear optical properties of TAA based EO chromophores and overcome some drawbacks of this type of chromophore, we utilized the MOPAC package combining AM1 and TDHF methods to directly compute molecular hyperpolarizabilities at 1907 nm (β_{1907}) and dipole moments of previously reported chromophores and carefully designed model chromophores.

The special structure of TAA, a three-bladed propeller structure with a planar or nearly planar central NCCC moiety, and the flexible rotations of the three phenyl rings, affords many design variants to test. A series of model chromophores with different numbers and positions of methoxy groups in the TAA donor moiety were systematically studied. Our calculation results show both substituent effects and conformational effects impact the EO properties of the chromophores. Electron donor substituent effects can increase the electron density of the substituted phenyl rings of the TAA moiety. The conformational factors significantly impact the π - π interactions among the lone pair of the central nitrogen atom, the p orbitals of the phenyl rings, and the lone pair of oxygen atoms in substituent groups. Frontier molecular orbital analysis reveals that a larger torsion angle between phenyl ring B or ring C and the central NCCC plane results in a reduced delocalization of the lone pair of the central N atom into phenyl ring B or ring C, which enhances the hyperpolarizability of the chromophore. On the other hand, with an increase of the torsion angle between phenyl ring B or ring C and the central NCCC plane, the delocalization of the lone pair of oxygen atoms in electron donor groups into the central N atom decreases, which reduces the electron donor effect. Chromophore 15 and 20 have the largest torsion angles between phenyl ring B or ring C and the central NCCC plane, which results in no or little electron donor effect from oxygen atoms of *ortho*-substituted methoxy groups.

Ortho-substitution dramatically affects the molecular conformations of the TAA moiety by steric effects and has a larger influence on hyperpolarizabilities and dipole moments of NLO chromophores than does *para*-substitution. Previous studies showed that compounds having methoxy groups in the *ortho* positions of ring B and ring C exhibit reduced charge-transport properties with respect to compounds containing methoxy groups in *para* positions of ring B and ring C.¹⁵ *Ortho*-substituted TAA chromophore can overcome some drawbacks of this class of chromophore. Introduction of additional methoxy groups in the *ortho* and *para* positions of ring B and ring C of the TAA moiety give higher hyperpolarizability values. Introduction of methoxy group on the *meta* position of ring A also can increase the hyperpolarizability and dipole moment.

Combining all our discoveries, chromophore 22 with a total of seven methoxy groups substituted on all *ortho* and *para* positions of ring B and ring C and on one *meta* position of ring A in the TAA moiety gives the highest β_{1907} value of all designed methoxy group substituted model molecules, which is 79% higher than its unsubstituted analogue 3. Both electron donor

substituent effects and steric conformation contribute to this large increase in hyperpolarizability. Further increases in both hyperpolarizability and dipole moment were achieved by replacing methoxy groups with better electron donor dimethylamino groups, on the *para* positions of chromophore 22.

Our calculation results give a theoretical basis to understand the relationship of structure and nonlinear properties of TAA based NLO chromophores. With careful consideration of steric and electronic factors, we can design and synthesize novel TAA based chromophores that overcome the current drawbacks and maintain high thermal stability to meet practical device requirements.

Acknowledgements

We gratefully acknowledge the Welch Foundation and the University of Texas at Dallas for their generous funding. We also wish to thank Shawna Liff for her guidance and Intel Corporation for their financial support.

References

- 1 F. Kajzar, K. S. Lee and A. K. Y. Jen, *Adv. Polym. Sci.*, 2003, **161**, 1–85.
- 2 S. R. Marder, B. Kippelen, A. K. Y. Jen and N. Peyghambarian, *Nature*, 1997, **388**, 845–851.
- 3 L. R. Dalton, W. H. Steier, B. H. Robinson, C. Zhang, A. Ren, S. Garner, A. T. Chen, T. Londergan, L. Irwin, B. Carlson, L. Fifield, G. Phelan, C. Kincaid, J. Amend and A. Jen, *J. Mater. Chem.*, 1999, **9**, 1905–1920.
- 4 B. A. Block, T. R. Younkin, P. S. Davids, M. R. Reshotko, P. Chang, B. M. Polishak, S. Huang, J. Luo and A. K. Y. Jen, *Opt. Express*, 2008, **16**, 18326–18333.
- 5 L. R. Dalton, P. A. Sullivan, D. Bale, B. Olbricht, J. Davies, S. Benight, I. Kosilkin, B. H. Robinson, B. E. Eichinger and A. K. Y. Jen, *Organic Thin Films for Photonic Applications*, 2010, **1039**, 13–33.
- 6 M. J. Cho, D. H. Choi, P. A. Sullivan, A. J. P. Akelaitis and L. R. Dalton, *Prog. Polym. Sci.*, 2008, **33**, 1013–1058.
- 7 P. A. Sullivan and L. R. Dalton, *Acc. Chem. Res.*, 2010, **43**, 10–18.
- 8 L. R. Dalton, P. A. Sullivan and D. H. Bale, *Chem. Rev.*, 2010, **110**, 25–55.
- 9 J. D. Luo, X. H. Zhou and A. K. Y. Jen, *J. Mater. Chem.*, 2009, **19**, 7410–7424.
- 10 J. A. Davies, A. Elangovan, P. A. Sullivan, B. C. Olbricht, D. H. Bale, T. R. Ewy, C. M. Isborn, B. E. Eichinger, B. H. Robinson, P. J. Reid, X. Li and L. R. Dalton, *J. Am. Chem. Soc.*, 2008, **130**, 10565–10575.
- 11 Z. W. Shi, J. D. Luo, S. Huang, B. M. Polishak, X. H. Zhou, S. Liff, T. R. Younkin, B. A. Block and A. K. Y. Jen, *J. Mater. Chem.*, 2012, **22**, 951–959.
- 12 L. Dalton, *Adv. Polym. Sci.*, 2002, **158**, 1–86.
- 13 S. M. Budy, S. Suresh, B. K. Spraul and D. W. Smith, *J. Phys. Chem. C*, 2008, **112**, 8099–8104.

- 14 Y. J. Cheng, J. D. Luo, S. Hau, D. H. Bale, T. D. Kim, Z. W. Shi, D. B. Lao, N. M. Tucker, Y. Q. Tian, L. R. Dalton, P. J. Reid and A. K. Y. Jen, *Chem. Mater.*, 2007, **19**, 1154–1163.
- 15 S. Suresh, H. Zengin, B. K. Spraul, T. Sassa, T. Wada and D. W. Smith, *Tetrahedron Lett.*, 2005, **46**, 3913–3916.
- 16 B. K. Spraul, S. Suresh, T. Sassa, M. A. Herranz, L. Echegoyen, T. Wada, D. Perahia and D. W. Smith, *Tetrahedron Lett.*, 2004, **45**, 3253–3256.
- 17 Y. Ji, Y. Qian and W. Lu, *J. Mater. Chem.*, 2012, **22**, 12375–12380.
- 18 E. M. Breitung, C.-F. Shu and R. J. McMahon, *J. Am. Chem. Soc.*, 2000, **122**, 1154–1160.
- 19 X. Ma, F. Ma, Z. Zhao, N. Song and J. Zhang, *J. Mater. Chem.*, 2010, **20**, 2369–2380.
- 20 X. Ma, F. Ma, Z. Zhao, N. Song and J. Zhang, *J. Mater. Chem.*, 2009, **19**, 2975–2985.
- 21 M. Blanchard-Desce, V. Alain, P. V. Bedworth, S. R. Marder, A. Fort, C. Runser, M. Barzoukas, S. Lebus and R. Wortmann, *Chem.–Eur. J.*, 1997, **3**, 1091–1104.
- 22 J.-M. Raimundo, P. Blanchard, N. Gallego-Planas, N. Mercier, I. Ledoux-Rak, R. Hierle and J. Roncali, *J. Org. Chem.*, 2001, **67**, 205–218.
- 23 J. Hung, W. Liang, J. Luo, Z. Shi, A. K. Y. Jen and X. Li, *J. Phys. Chem. C*, 2010, **114**, 22284–22288.
- 24 M. He, T. M. Leslie and J. A. Sinicropi, *Chem. Mater.*, 2002, **14**, 4662–4668.
- 25 K. Schmidt, S. Barlow, A. Leclercq, E. Zojer, S.-H. Jang, S. R. Marder, A. K. Y. Jen and J.-L. Bredas, *J. Mater. Chem.*, 2007, **17**, 2944–2949.
- 26 X. Piao, X. Zhang, S. Inoue, S. Yokoyama, I. Aoki, H. Miki, A. Otomo and H. Tazawa, *Org. Electron.*, 2011, **12**, 1093–1097.
- 27 O. Kwon, S. Barlow, S. A. Odom, L. Beverina, N. J. Thompson, E. Zojer, J.-L. Brédas and S. R. Marder, *J. Phys. Chem. A*, 2005, **109**, 9346–9352.
- 28 Z.-Y. Hu, A. Fort, M. Barzoukas, A. K. Y. Jen, S. Barlow and S. R. Marder, *J. Phys. Chem. B*, 2004, **108**, 8626–8630.
- 29 M. He, T. M. Leslie and J. A. Sinicropi, *Chem. Phys.*, 2002, **14**, 2393–2400.
- 30 I. Reva, L. Lapinski, N. Chattopadhyay and R. Fausto, *Phys. Chem. Chem. Phys.*, 2003, **5**, 3844–3850.
- 31 P. Cias, C. Slugovc and G. Gescheidt, *J. Phys. Chem. A*, 2011, **115**, 14519–14525.
- 32 A. K. Mandal, M. Suresh, P. Das and A. Das, *Chem.–Eur. J.*, 2012, **18**, 3906–3917.
- 33 R. Glaser, J. F. Blount and K. Mislow, *J. Am. Chem. Soc.*, 1980, **102**, 2777–2786.
- 34 G. Meijer, G. Berden, W. L. Meerts, H. E. Hunziker, M. S. de Vries and H. R. Wendt, *Chem. Phys.*, 1992, **163**, 209–222.
- 35 A. N. Sobolev, V. K. Belsky, I. P. Romm, N. Y. Chernikova and E. N. Guryanova, *Acta Crystallogr., Sect. C: Cryst. Struct. Commun.*, 1985, **41**, 967–971.
- 36 B. Kelly, J. Tanski, M. Anzovino and G. Parkin, *J. Chem. Crystallogr.*, 2005, **35**, 969–981.
- 37 <http://www.cambridgesoft.com/>.
- 38 S. P. Karna and M. Dupuis, *J. Comput. Chem.*, 1991, **12**, 487–504.
- 39 W. Humphrey, A. Dalke and K. Schulten, *J. Mol. Graphics*, 1996, **14**, 33–38.
- 40 M. J. Frisch, H. B. Schlegel, G. E. Scuseria, M. A. Robb, J. R. Cheeseman, J. A. Montgomery Jr, T. Vreven, K. N. Kudin, J. C. Burant, J. M. Millam, S. S. Iyengar, J. Tomasi, V. Barone, B. Mennucci, M. Cossi, G. Scalmani, N. Rega, G. A. Petersson, H. Nakatsuji, M. Hada, M. Ehara, K. Toyota, R. Fukuda, J. Hasegawa, M. Ishida, T. Nakajima, Y. Honda, O. Kitao, H. Nakai, M. Klene, X. Li, J. E. Knox, H. P. Hratchian, J. B. Cross, V. Bakken, C. Adamo, J. Jaramillo, R. Gomperts, R. E. Stratmann, O. Yazyev, A. J. Austin, R. Cammi, C. Pomelli, J. W. Ochterski, P. Y. Ayala, K. Morokuma, G. A. Voth, P. Salvador, J. J. Dannenberg, V. G. Zakrzewski, S. Dapprich, A. D. Daniels, M. C. Strain, O. Farkas, D. K. Malick, A. D. Rabuck, K. Raghavachari, J. B. Foresman, J. V. Ortiz, Q. Cui, A. G. Baboul, S. Clifford, J. Cioslowski, B. B. Stefanov, G. Liu, A. Liashenko, P. Piskorz, I. Komaromi, R. L. Martin, D. J. Fox, T. Keith, M. A. Al-Laham, C. Y. Peng, A. Nanayakkara, M. Challacombe, P. M. W. Gill, B. Johnson, W. Chen, M. W. Wong, C. Gonzalez and J. A. Pople, *Gaussian 03, Revision C.02*, Gaussian, Inc., Wallingford CT, 2004.
- 41 T. Kinnibrugh, S. Bhattacharjee, P. Sullivan, C. Isborn, B. H. Robinson and B. E. Eichinger, *J. Phys. Chem. B*, 2006, **110**, 13512–13522.

Electronic supplementary information (ESI)

Towards an understanding of structure-nonlinearity relationships in triarylamine-based push-pull electro-optic chromophores: the influence of substituent and molecular conformation on molecular hyperpolarizabilities

Jingbo Wu, Blake A. Wilson, Dennis W. Smith, Jr., and Steven O. Nielsen*

*Department of Chemistry and the Alan G. MacDiarmid NanoTech Institute,
The University of Texas at Dallas, Richardson TX 75080, USA*

1. Comparison of the trends in hyperpolarizability predicted by our calculations with experimental data.

For EO chromophores with different electron acceptors **4**, **5**, and **6**, our calculations show hyperpolarizabilities increase in the order of **4** ($\beta_{1907} = 147 \times 10^{-30}$ esu) < **5** ($\beta_{1907} = 178 \times 10^{-30}$ esu) < **6** ($\beta_{1907} = 280 \times 10^{-30}$ esu). The hyperpolarizability β values of these three chromophores were measured experimentally at 802 nm in CHCl_3 . Chromophore **4** has the lowest β value ($\beta_{802} = 1000 \times 10^{-30}$ esu), then chromophore **5** ($\beta_{802} = 5000 \times 10^{-30}$ esu), and chromophore **6** has the highest β value ($\beta_{802} = 20,000 \times 10^{-30}$ esu); the order from experimental data is **4** < **5** < **6**.¹

For EO chromophores with different numbers of methoxy groups on *para* positions of the TAA moiety **7**, **8**, and **9**, our calculations show hyperpolarizabilities increase in the order of **7** ($\beta_{1907} = 321 \times 10^{-30}$ esu) < **8** ($\beta_{1907} = 342 \times 10^{-30}$ esu) < **9** ($\beta_{1907} = 358 \times 10^{-30}$ esu). The hyperpolarizability β values of these three chromophores were measured experimentally at 1907 nm in CHCl_3 . Chromophore **7** has the lowest β value ($\beta_{1907} = 1770 \pm 89 \times 10^{-30}$ esu), then chromophore **8** ($\beta_{1907} = 2150 \pm 259 \times 10^{-30}$ esu), and chromophore **9** has the highest β value ($\beta_{802} = 3456 \pm 128 \times 10^{-30}$ esu); the order from experimental data is **7** < **8** < **9**.²

The trends in hyperpolarizability predicted from our calculations match the trends from experimental data.

2. Methoxy group substituted NLO chromophores

2.1. Polarizability (α_{average}), second-order polarizability (β), energy and dipole moment (μ).

ESI-Table 1 lists the average polarizability (α_{average}), second-order polarizability (β), energy, and dipole moment (μ) of the model NLO chromophores and natural triarylamine molecule.

We found the NLO chromophores with the same number of methoxy groups on the TAA moiety have similar α_{average} values no matter where the methoxy group is located. For example, mono-methoxy substituted NLO chromophores, 10-14, have similar α_{average} values around 420

a.u. and the α_{average} values of di-methoxy substituted NLO chromophores are around 444 a.u. Introduction of more methoxy group on the TAA moiety enhances the α_{average} values.

A detailed discussion of second-order polarizability (β) is found in the main paper. Briefly, introduction of several methoxy groups on appropriate locations of the TAA moiety can dramatically increase the second-order polarizability of the NLO chromophore.

Stronger electron acceptor groups have lower total energy when they have the same electron donor and bridge (cf. **4** > **5** > **6** > **9**). Introducing more methoxy groups on the TAA moiety causes the total energy to decrease (cf. **8** > **9**; **1**~**3** > **10** ~ **14** > **4**, **15**~**18** > **19**, **20** > **21** > **22**). NLO chromophores with the same number of methoxy group on the TAA moiety have similar total energy no matter where the methoxy groups are located. The difference in the HOMO and LUMO energies of all models is very small. Model chromophore **22** has the highest HOMO and LUMO energy of all model chromophores. Chromophores with the strongest electron acceptor ($\text{CF}_3\text{-Ph-TCF}$) have the lowest LUMO energy. And model **13** with di-*ortho* substituted methoxy groups on the phenyl ring connected with the bridge and electron acceptor group has the lowest HOMO energy. Chromophores with four methoxy groups on the *ortho* positions of ring B and ring C (**19**, **21** and **22**) have higher HOMO energies, which may be due to steric effects.

The average dipole moments (μ) are from 0.019 Debye (natural TAA) to 13.59 Debye (**model 9**). Model chromophores with stronger electron acceptors have larger dipole moment μ values (cf. **4** < **6** < **9**). Introduction of a methoxy group on the *ortho* positions of ring B and ring C can effectively increase the dipole moment. Model chromophore **22** with the largest number of methoxy groups on the TAA moiety has the largest dipole moment of models with the same bridge and electron acceptor.

2.2. C-N bond lengths and torsion angles

The bond lengths between the central nitrogen atom and the carbon atoms of the three phenyl rings are listed in table 2. The Ph-N bond lengths are indicative of the delocalization of the nitrogen lone pair into the aryl ring. Except for model **13** and model **17**, the bond length ($\text{C-N}_{\text{ring A}}$) between the central nitrogen and the phenyl ring which connects with the bridge and electron acceptor is shorter than the bond lengths ($\text{C-N}_{\text{ring B}}$ and $\text{C-N}_{\text{ring C}}$) between the central nitrogen and the other two phenyl rings. The difference in model **13** and model **17** is that phenyl ring A rotates out of the central NCCC reference plane because of steric effects, and the nitrogen lone pair predominately delocalizing into the other two phenyl rings. Model chromophores with different electron acceptors (**4**, **5**, **6**, **7-9**) have similar values in the $\text{C-N}_{\text{ring A}}$ bond length. The $\text{C-N}_{\text{ring A}}$ bond lengths of model chromophore **15** and **20** are the shortest of all studied model chromophores, which also have the smallest torsion angle $\angle A$ (around 3°) and the largest torsion angles $\angle B$ and $\angle C$. In model chromophores **15** and **20**, the nitrogen lone pair predominately delocalizes into ring A due to the molecular conformational effect.

The three torsion angles between the central NCCC reference plane and the three phenyl rings, respectively, are listed in ESI-table 2. The torsion angles are important parameters to quantitatively measure the molecular conformations of the TAA moiety and help us to

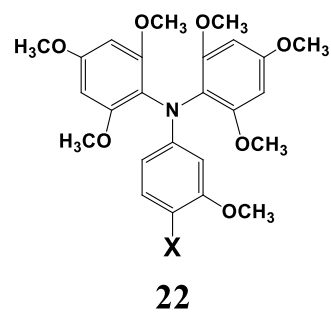
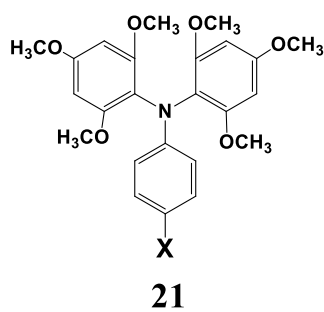
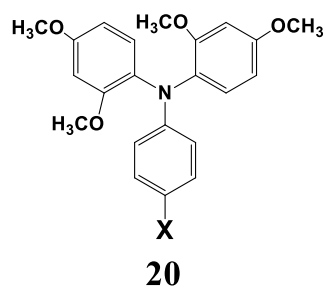
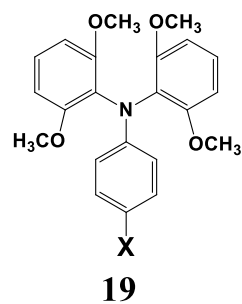
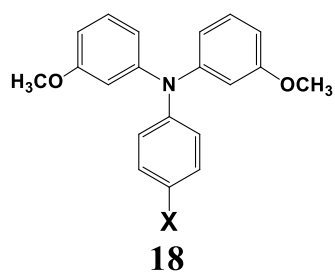
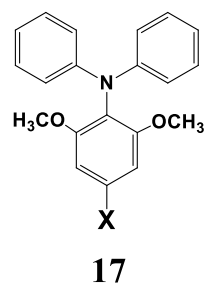
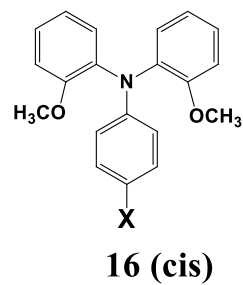
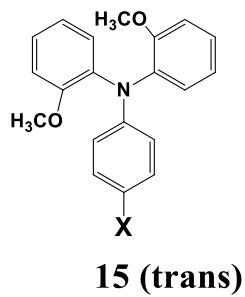
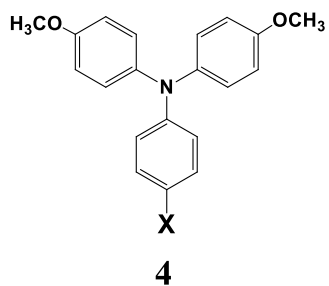
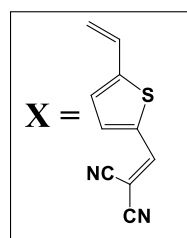
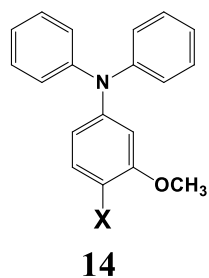
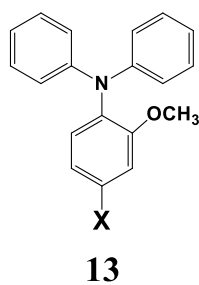
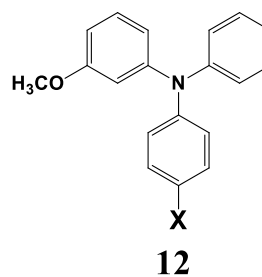
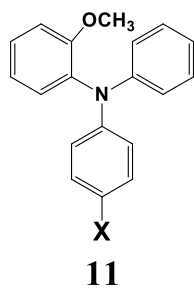
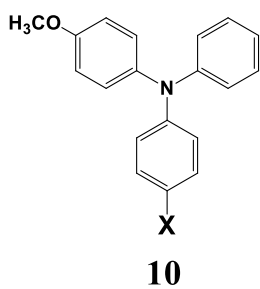
understand the delocalization of the nitrogen lone pair into the three phenyl rings. The natural triarylamine molecule is symmetrical and has torsion angles of about 35° . Introduction of methoxy groups on the *para* positions of ring B and ring C causes slight changes in all three torsion angles. Introduction of methoxy groups on the *ortho* positions of ring B and ring C causes dramatic changes in all three torsion angles. All these changes lead to larger delocalization of the nitrogen lone pair into ring A which connects with the thiophene bridge and electron acceptor and less delocalization of the central nitrogen lone pair into the other two rings.

ESI-Table 1. The polarizabilities (a.u.), second-order polarizabilities (10^{-30} esu), energy and dipole moment (μ) of designed NLO chromophores and the natural triphenylamine molecule.

model	α_{average} (au)	β_{1907} (10^{-30} esu)	HOMO (EV)	LUMO (EV)	Total Energy (EV)	μ (Debye)
1	398	105	-7.989	-1.665	-4656.80026	5.317
2	403	114	-8.002	-1.641	-4656.80439	5.949
3	406	121	-8.041	-1.638	-4656.76928	6.889
4	449	147	-7.933	-1.587	-5608.46515	8.142
5	545	178	-7.921	-1.7	-7222.3705	7.497
6	589	280	-7.962	-2.091	-7254.57921	11.164
7	607	321	-8.061	-2.323	-8384.17799	11.381
8	630	342	-7.977	-2.321	-8860.04062	12.324
9	649	358	-7.974	-2.289	-9335.8765	13.59
10	427	131	-7.963	-1.621	-5132.61544	6.629
11	420	131	-8.065	-1.531	-5132.50926	8.392
12	421	104	-8.082	-1.643	-5132.62793	5.529
13	415	69	-8.229	-1.679	-5132.43179	5.701
14	426	127	-8.031	-1.52	-5132.599	8.534
15	441	172	-7.916	-1.453	-5608.25595	9.918
16	444	159	-7.875	-1.491	-5608.16847	9.827
17	432	43	-7.988	-1.788	-5608.1577	2.624
18	444	111	-8.082	-1.652	-5608.47797	6.616
19	481	183	-7.682	-1.4	-6559.57179	12.368
20	482	185	-7.894	-1.443	-6560.01286	10.343
21	522	199	-7.613	-1.381	-7511.30433	12.482
22	543	216	-7.58	-1.281	-7987.14361	13.288
TAA	225	0.05	-7.956	0.179	-2715.96049	0.019
23	449	146	-7.78	-1.581	-5188.41714	8.727
24	441	131	-7.977	-1.556	-5188.29214	8.105
25	438	99	-8.029	-1.558	-5188.33941	7.379
26	491	174	-7.673	-1.515	-5720.06225	10.603
27	478	161	-7.984	-1.501	-5719.70182	8.483
28	562	221	-7.742	-1.439	-6783.08678	10.679
29	632	216	-7.334	-1.399	-7845.69969	10.398
30	523	188	-7.904	-1.452	-6671.57933	11.11
31	566	242	-7.397	-1.308	-7622.85714	15.45
32	586	247	-7.408	-1.203	-8098.70935	17.11

ESI-Table 2: The bond lengths between the central nitrogen and the carbon atom of the three phenyl rings of the TAA donor moiety and the torsion angles between the central NCCC plane and the three phenyl rings of the TAA moiety.

model	C-N bond (Å) Ra	C-N bond (Å) Rb	C-N bond (Å) Rc	∠ A	∠ B	∠ C
				Ring A	Ring B	Ring C
1	1.409	1.414	1.416	31.58	35.68	37.15
2	1.408	1.416	1.417	29.94	36.32	37.9
3	1.408	1.415	1.417	30.68	35.56	37.87
4	1.406	1.421	1.421	21.73	45.77	47.46
5	1.405	1.419	1.42	24.45	44.71	43.91
6	1.407	1.421	1.42	24.06	45.29	44.62
7	1.408	1.415	1.416	30.55	36.16	37.41
8	1.406	1.418	1.415	28.05	41.77	37.18
9	1.407	1.422	1.421	22.82	45.88	47.23
10	1.406	1.418	1.415	27.06	42.52	37.83
11	1.408	1.426	1.423	17.89	79.02	48.08
12	1.409	1.414	1.416	31.92	34.94	37.57
13	1.421	1.422	1.422	51.41	35.42	35.22
14	1.407	1.416	1.416	28.75	38.27	38.45
15	1.396	1.422	1.423	2.58	84.95	89.54
16	1.403	1.421	1.423	16	54.78	62.04
17	1.418	1.414	1.409	85.79	36.17	29.26
18	1.41	1.414	1.415	33.15	34.77	35.51
19	1.404	1.419	1.417	15.9	62.04	56.45
20	1.397	1.423	1.424	2.81	84.6	86.12
21	1.404	1.418	1.42	15.03	56.56	64.96
22	1.401	1.417	1.418	16.78	57.56	64.86
TAA	1.413	1.413	1.413	34.31	34.36	35.15
23	1.406	1.419	1.414	26.94	42.72	37.55
24	1.407	1.423	1.414	27.32	60.25	34.73
25	1.41	1.415	1.415	30.81	37.14	36.79
26	1.406	1.423	1.423	19.55	49.42	49.68
27	1.405	1.418	1.418	7.45	62.53	75.59
28	1.39	1.423	1.423	4.2	75.05	77.37
29	1.407	1.417	1.417	35.3	49.32	49.48
30	1.402	1.427	1.426	4.75	86.58	80.03
31	1.402	1.418	1.42	13.36	56.74	66.58
32	1.401	1.419	1.42	12.55	57.24	67.04



ESI-Scheme one: the structures of chromophore **4** and **10-22**.

3. Dimethylamino substituted TAA based chromophores 23-29

Based on our discoveries on methoxy substituted chromophores, a series of dimethylamino substituted TAA based chromophores were designed and studied. Three important positions on the three phenyl rings were studied: the *para* and *ortho* positions on ring B and ring C and the *meta* position on ring A. Chromophores with different numbers (1, 2, 4, and 6) of dimethylamino groups on the three phenyl rings were investigated.

Because the dimethylamino group is a stronger electron donor group than the methoxy group, mono- and di-*para*-dimethylamino substituted chromophores display higher β_{1907} values than that of methoxy substituted analogues. [cf. **23** ($\beta_{1907} = 146 \times 10^{-30}$ esu) vs. **10** ($\beta_{1907} = 131 \times 10^{-30}$ esu) and **4** ($\beta_{1907} = 147 \times 10^{-30}$ esu) vs. **26** ($\beta_{1907} = 174 \times 10^{-30}$ esu)].

Introduction of dimethylamino groups on the *ortho* position(s) of the TAA moiety also can cause molecular conformational changes due to steric effects. However, the conformational effect is less than that of the methoxy group, because the torsion angles between ring B or ring C and the central CCCN plane are smaller than their methoxy group substituted counterparts. [cf. **11** ($\angle B = 79^\circ$) vs **24** ($\angle B = 63^\circ$), **15** ($\angle B = 85^\circ$ and $\angle C = 90^\circ$) vs **27** ($\angle B = 63^\circ$ and $\angle C = 76^\circ$), and **20** ($\angle B = 85^\circ$ and $\angle C = 86^\circ$) vs. **28** ($\angle B = 75^\circ$ and $\angle C = 77^\circ$)].

Introduction of a dimethylamino group on the *meta* position of ring A yields a large decrease in hyperpolarizability (cf. **25** vs **3**). This may be because the steric effect of the larger dimethylamino group compromises the planarity of the conjugated system of phenyl ring A, bridge, and electron acceptor, resulting in the decrease in hyperpolarizability.

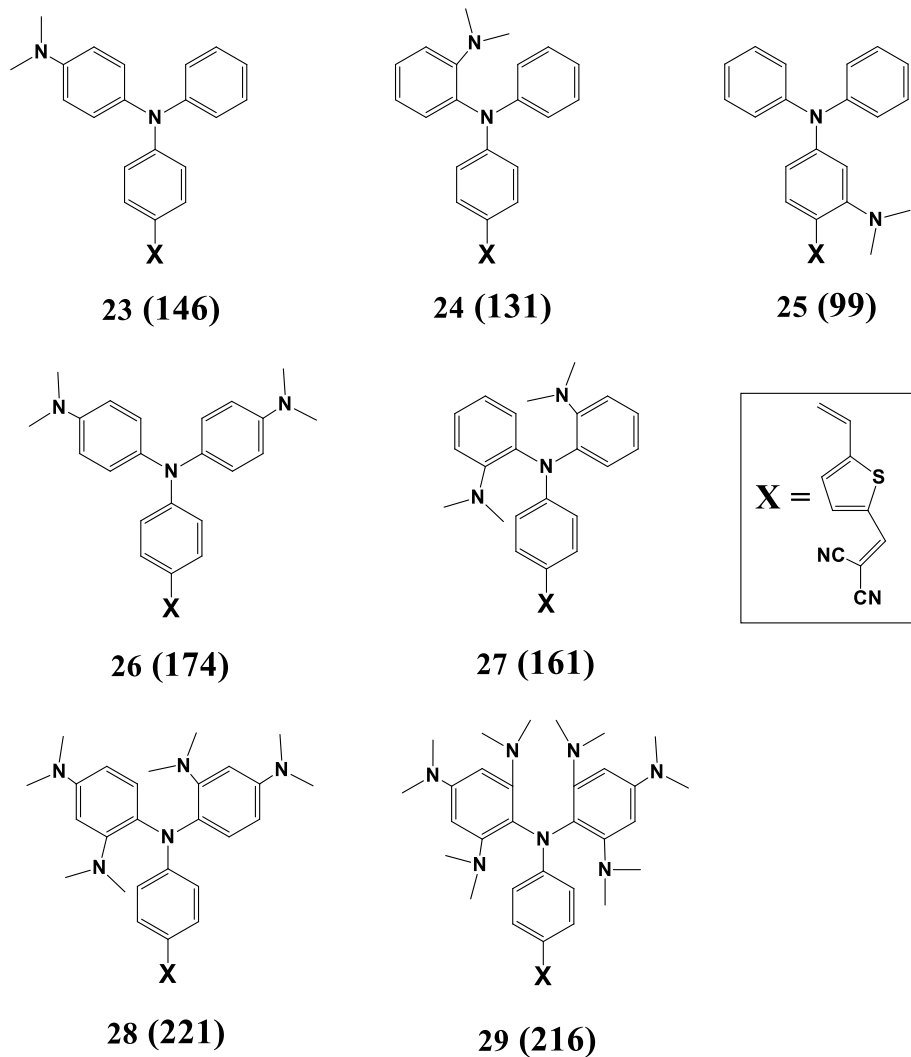
Fig SI-1 shows isosurfaces of the HOMO for di-substituted chromophore **27**. There are small contributions from the lone pair electrons on the nitrogen atoms in *ortho*-substituted dimethylamino groups on phenyl ring B and ring C. Both the electron donor effect and molecular conformational effect contribute to the increase in hyperpolarizability compared to nonsubstituted TAA chromophore **3**.

Introducing more dimethylamino groups onto the TAA moiety yield a large increase in hyperpolarizability (cf. **26** vs **28**). Chromophore **28**, with two dimethylamino groups on *ortho* positions and two methoxy groups on *para* positions of ring B and C of the TAA donor moiety, respectively, has the largest β_{1907} value ($\beta_{1907} = 221 \times 10^{-30}$ esu). As we discussed in the main paper, both an electronic donor effect and molecular conformational effect contribute to this increase in hyperpolarizability. Fig SI-1 also plots isosurfaces of the HOMO for di-substituted chromophore **28**. There are small contributions from the lone pair electrons on the nitrogen atoms in *ortho*-substituted dimethylamino groups on phenyl ring B and ring C.

Dimethylamino substituted chromophore **28** has a larger β_{1907} value than its methoxy substituted counterpart, chromophore **22** (cf. **28**, $\beta_{1907} = 221 \times 10^{-30}$ esu vs. **22**, $\beta_{1907} = 216 \times 10^{-30}$ esu), however, chromophore **22** has a much larger dipole moment than chromophore **28** (cf. **22**, $\mu = 13.3$ D vs **28**, $\mu = 10.7$ D). Introduction of methoxy groups on the *ortho* position of the TAA moiety has larger effect on the molecular dipole moment than that of dimethylamino groups.

Overall, introduction of dimethylamino groups on both *para* and *ortho* positions of ring B and ring C of the TAA moiety can effectively improve the hyperpolarizability (cf. **28** and **29**). *Ortho*

substitution can affect the molecular conformations of the TAA moiety by a steric effect. However, this effect is less than their methoxy substituted counterparts. *Ortho* dimethylamino substitution has less effect on the dipole moment than *ortho* methoxy substitution. Introduction of a dimethylamino group on the *meta* position of ring A causes a large decrease in hyperpolarizability.



ESI-Scheme two: the structures of dimethylamino substituted TAA based chromophores.

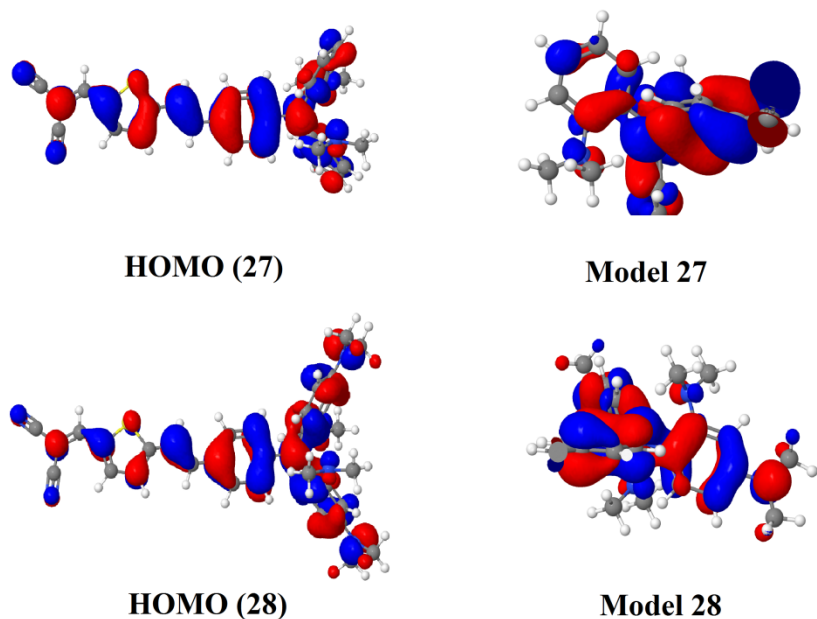
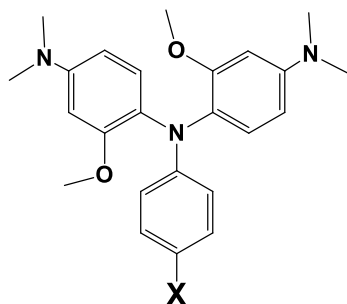


Figure S-1. The frontier molecular orbitals (HOMO and LUMO) of model NLO chromophores **27** and **28** (left); and isosurfaces of the HOMO for phenyl ring B or phenyl ring C in the TAA moiety of model NLO chromophores **27** and **28** (right).

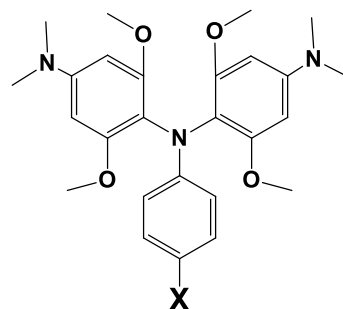
4. The hybrid substituted TAA based chromophores

Because the dimethylamino group is a better electron donor than the methoxy group, and because the methoxy group is a better group to control the molecular conformation than the dimethylamino group, we designed several hybrid substituted model chromophores with two dimethylamino groups on the *para* positions of ring B and ring C and different numbers of methoxy groups on other important positions.

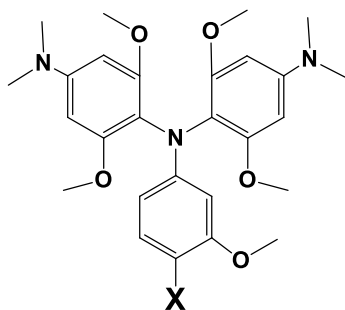
Further increases in both hyperpolarizability and dipole moment were achieved by replacing methoxy groups with dimethylamino groups on the *para* positions of chromophore **22** (cf. **22**, $\beta_{1907} = 216 \times 10^{-30}$ esu vs **32**, $\beta_{1907} = 247 \times 10^{-30}$ esu) and (cf. **22**, $\mu = 13.3$ D vs **32**, $\mu = 17.1$ D). Chromophore **32** with two dimethylamino groups on the *para* positions of ring B and ring C, four methoxy groups on the *ortho* positions of ring B and ring C, and one methoxy group on the *meta* position of ring A gives the highest hyperpolarizability and dipolar moment of all designed model molecules. The β_{1907} value of chromophore **32** is 104% higher than its unsubstituted analogue **3** (cf. **3**, $\beta_{1907} = 121 \times 10^{-30}$ esu vs **32**, $\beta_{1907} = 247 \times 10^{-30}$ esu).



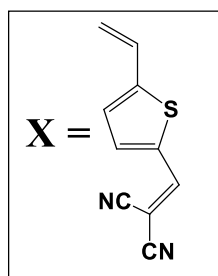
30 (188)



31 (242)



32 (247)



ESI-Scheme three: the structures of hybrid substituted TAA based chromophores.

1. B. K. Spraul, S. Suresh, T. Sassa, M. A. Herranz, L. Echegoyen, T. Wada, D. Perahia and D. W. Smith, *Tetrahedron Lett*, 2004, 45, 3253-3256.
2. Y. J. Cheng, J. D. Luo, S. Hau, D. H. Bale, T. D. Kim, Z. W. Shi, D. B. Lao, N. M. Tucker, Y. Q. Tian, L. R. Dalton, P. J. Reid and A. K. Y. Jen, *Chem Mater*, 2007, 19, 1154-1163.

School of Natural Sciences and Mathematics

2014-02-17

Towards an Understanding of Structure-Nonlinearity Relationships in Triarylamine-based Push-Pull Electro-Optic Chromophores: The Influence of Substituent and Molecular Conformation on Molecular Hyperpolarizabilities

UTD AUTHOR(S): Jingbo Wu, Blake A. Wilson, Dennis W. Smith, Jr. and Steven O. Nielsen

©2014 The Royal Society of Chemistry